Infrared spectra of individual semiconducting single-walled carbon nanotubes: Testing the scaling of transition energies for large diameter nanotubes

Matthew Y. Sfeir and James A. Misewich*
Condensed Matter Physics and Materials Science, Brookhaven National Laboratory, Upton, New York 11973, USA

Sami Rosenblatt, Yang Wu, Christophe Voisin,† Hugen Yan, Stéphane Berciaud, and Tony F. Heinz
Departments of Physics and Electrical Engineering, Columbia University, New York, New York 10027, USA

Bhupesh Chandra, Robert Caldwell, Yuyao Shan, and James Hone
Department of Mechanical Engineering, Columbia University, New York, New York 10027, USA

G. L. Carr
National Synchrotron Light Source, Brookhaven National Laboratory, Upton, New York 11973, USA
(Received 1 September 2010; published 11 November 2010)

We have measured the low-energy excitonic transitions of chiral assigned individual large-diameter semiconducting single-walled nanotubes using a high-resolution Fourier transform photoconductivity technique. When photoconductivity is complemented by Rayleigh scattering spectroscopy, as many as five optical transitions can be identified on the same individual nanotube over an energy range of 0.3–2.7 eV. We find that well-established energy scaling relations developed for nanotubes of smaller diameter are not consistent with the measured low-energy transitions in large (1.8–2.3 nm) diameter nanotubes.

DOI: 10.1103/PhysRevB.82.195424 PACS number(s): 78.67.Ch, 73.22.−f, 73.63.Fg, 78.30.Na

I. INTRODUCTION

Many advances have recently been made in the optical characterization of single-walled carbon nanotubes (SWNTs), including the development of sensitive techniques for the investigation of individual nanotubes.[1–4] However, little experimental data has been available for well-defined nanotubes out to the midinfrared spectral region. As a consequence, there is a significant deficiency in our experimental knowledge of the position and characteristics of electronic transitions of semiconducting SWNTs of moderate diameter since their fundamental (E_{11}) and second (E_{22}) transitions lie in the near to mid-infrared. This represents a crucial gap in our understanding of the basic electronic structure of nanotubes in a size regime that is prevalent in typical syntheses and whose properties and applications have been widely studied.[5] Further, characterization of these electronic transitions offers an excellent testing ground for models of the optically excited states in nanotubes, a subject of considerable interest and uncertainty.[6,7] Progress has recently been made on obtaining spectral information in the near and mid-IR using optoelectronic techniques, including measurements of resonances in the AC displacement current and photoconductivity.[8–10] However, the interpretation of spectral information has been hindered by lack of knowledge of the crystallographic structure of the nanotubes under study.

Here we report infrared optical transitions of individual SWNTs of defined crystallographic structure, i.e., of known chiral index. The infrared spectroscopy was carried out at the individual nanotube level using a new method of Fourier transform photoconductivity (FTPC) spectroscopy. In this fashion we are able to access the lowest-lying (E_{11}) and second (E_{22}) exciton transitions in semiconducting nanotubes. The chiral indices of the individual nanotubes under investigation were obtained from measurements of higher-lying optical transitions using Rayleigh scattering spectroscopy and previously developed spectroscopic assignments.[11] Taken together these two techniques provide unique spectroscopic data, including identification of up to five distinct electronic transitions in individual semiconducting SWNTs. The results permit us to examine the dependence of the optical transition energies on the nanotube structure in a previously unexplored regime.

In particular, we assess the applicability of widely applied formalism based on zone folding of the graphene bands with many-body corrections to the measured infrared exciton transitions. This model is often referred to as the two-dimensional (2D) model, as its parameter represents electron-electron interactions that occur on length scales smaller than the nanotube circumference (as would be present in graphene).[12] It relies on the effective cancellation of two strong countervailing one-dimensional (1D) effects occurring on length scales comparable to the nanotube circumference: band-gap renormalization and exciton binding. In the resulting description, the transition energies are determined simply by the wave vector associated with the relevant subband transition (analogous to zone folding in a single-particle picture). The diameter of the nanotube is not in itself important: higher-lying subband transitions of large nanotubes are predicted to produce the same optical transition energy as lower subband transitions in nanotubes with appropriately increased diameter. This model has led to simple but accurate parameterization of the E_{11} and E_{22} transitions energies for a large class of nanotubes. Only for very small diameter nanotubes, where curvature effects become significant, has this approach been shown to fail.[13]

One would expect such a 2D model to be especially appropriate for nanotubes of larger diameter, which exhibit sig-

 ©2010 The American Physical Society

nificantly larger circumferences and radii of curvature and as a consequence, lower transition energies. This hypothesis has, however, never been tested experimentally. In fact, as we show below, no scaling relation using a single "2D" parameter can simultaneously explain our experiment results for the E_{11} and E_{22} transition energies in larger diameter nanotubes and the existing data on transitions in smaller diameter nanotubes. This breakdown of scaling is especially apparent when we compare our measured E_{22} energies for transitions of large diameter nanotubes with available data for the E_{11} energies of smaller diameter nanotubes with the same wavevector. This result implies that 1D many-body effects cannot be completely ignored.

II. EXPERIMENTAL DETAILS

In our experiments, single-walled nanotubes were initially grown across open slits by chemical vapor deposition.[14] In this geometry, SWNTs could be investigated by Rayleigh scattering spectroscopy, a technique that provides sensitivity to individual nanotubes through a determination of the frequency-dependent cross section for elastic light scattering.[4] In addition to unambiguously identifying individual nanotubes, as opposed to bundles or multiwalled nanotubes, the technique yielded spectra for the third (E_{33}) and fourth (E_{44}) subband transitions. Assignments of the nanotube chiral index were made by comparison to an accumulated database of optical spectra that has been organized following "family" behavior, the systematic evolution of the transition energies of a SWNT with changing structural parameters.[15] The assignments for these family trends had been previously established by performing spectroscopy of individual nanotubes with structures determined by electron diffraction.[11,16]

After completion of Rayleigh spectroscopy and identification of the chiral index of each nanotube, we prepared the sample for Fourier-transform photoconductivity measurements. This required transfer printing each nanotube onto a silicon wafer (300 nm oxide epilayer) and preparation of a SWNT field-effect transistor.[17] Source and drain electrodes, with spacings between 1 and 20 μm [Fig. 1(a)], were patterned by electron-beam lithography and lift-off of Cr/Au and Ti/Pd layers. The Cr and Ti layers, in addition to enhancing adhesion, produce large Schottky barriers and therefore strong and tunable electric fields at the nanotube-metal interface.[18] As shown in Fig. 1(b), the devices are weakly ambipolar (high *n*-type resistance >10 GΩ) with large contact barriers as inferred by a high (5 MΩ) on-state resistance and on/off ratio (10^5) for *p*-side conduction. High-contact resistance was found to be a necessary condition for the observation of photocurrent, consistent with the spectral evidence (discussed below) for excitonic absorptions.

FTPC experiments were performed using synchrotron radiation (National Synchrotron Light Source) coupled into a Fourier transform spectrometer and focused with an optical microscope. The Fourier transform technique permits measurement over a wide spectral range, with well-known improvements in speed (Fellget advantage) and noise (Jacquinot advantage) compared to conventional measurements with scanned excitation.[19] In the present study, the sample itself, i.e., an individual nanotube, serves as the photodetector. The photocurrent spectra were recorded in both rapid scan and "step-scan" modes utilizing a combination of transimpedance and lock-in amplifiers, and bench software. Typical spectra were collected in just a few seconds in the rapid scan configuration and several hundred scans are typically averaged together. In order to test that there are no shifting or damping of the peaks due to the RC response of the photoconductive circuit, step-scan spectra were collected with the light mechanically chopped at 100 Hz as the interferometer mirror was moved in discrete steps (64 cm^{-1} resolution). No change in the photocurrent spectra was detected. Alternatively, steady-state transport or time traces of the photocurrent were digitized and recorded using a data acquisition card.

During the FTPC measurements, the source-drain bias and the gate voltage were adjusted to obtain a strong photoresponse while minimizing the dark current. Figure 1(c) shows a time trace of the total current in the device with the light modulated at 100 Hz under bias conditions denoted by the arrow in Fig. 1(b). Under these conditions we obtained high-quality photoconductivity interferograms, an example of which is shown in of Fig. 1(d). The photocurrent excitation spectrum of the nanotube is obtained as the Fourier transform of the measured interferogram. The useful spectral range extended from photon energies of 0.25 to 1.25 eV, with a spectral resolution of 1 meV.

In order to properly normalize the photoconductivity spectra, it was necessary to determine the instrument and source characteristics. The spectral profile of the excitation light was determined using a pyroelectric detector (DTGS KBr), which has a flat broadband spectral response, placed at the focus of the microscope objective. The resulting spectrum includes the synchrotron, instrument, and beam splitter responses and was subsequently used to correct the photoconductivity spectra. The total power incident on the sample was too small to be measured with a thermal power meter and had to be estimated using a Si photodiode and a set of narrow bandpass filters (10 nm bandwidth, 50% transmission at 850 and 880 nm). Integrating these sections of the spectral profile with respect to the total curve gives an upper bound to the incident power of 1 mW corresponding to an irradiance of <700 W/cm^2 of broadband radiation in the excitation spot.

III. RESULTS AND DISCUSSION

The Fourier transform of the normalized interferogram yields the photocurrent excitation spectrum of the nanotube under study. Figures 2(a) and 2(b) show, respectively, FTPC spectra for a (14,13) nanotube (with a diameter of 1.9 nm) and for a (19,14) nanotube (with a diameter of 2.3 nm). Both of the FTPC spectra are quite simple in form, with two primary observed features that we assign to the E_{11} and E_{22} excitonic transitions. In addition to the requirements on device fabrication (which suggest excitonic resonances), there are several pieces of spectral evidence for this assignment. The first is that these peaks can be approximated by Lorent-

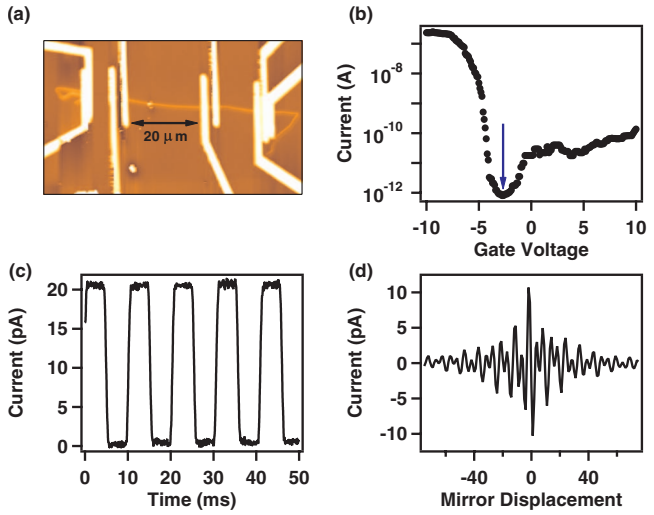

FIG. 1. (Color) (a) Large-field atomic force microscopy image (electrostatically enhanced) showing a 70 μm section of a transferred SWNT after characterization by resonant Rayleigh scattering. (b) Current vs. gate voltage characteristics of a typical transferred SWNT. The source-drain voltage is 1 V and the arrow indicates the gating conditions used for subsequent photoconductivity experiments. (c) Photocurrent time-trace under 100 Hz modulated broadband IR illumination and (d) the corresponding photocurrent interferogram in the same device.

zian line shapes and show no obvious asymmetry. In contrast, for a peak arising from a van Hove singularity at the band edge, an asymmetrical line shape would be expected. The excitonic nature of E_{11} transition and the lack of oscillator strength in possible interband transitions are fully compatible with earlier studies for smaller diameter nanotubes with transitions in the visible spectral range.[20,21] Furthermore, studies of enriched films of small diameter (7,5) SWNTs have recently shown identical E_{11} and E_{22} features in both photoconductivity and absorption, demonstrating that photocurrent can indeed be observed from excitons.[22] Finally, we have determined our dissociation efficiency to be $<1\%$, consistent with a field-ionization model for moderately bound excitons[23] which considers experimental estimates for the absorption cross section,[24] carrier lifetimes,[25,26] and Schottky barrier widths.[18] We note that nanotube photoexcitation spectra have been previously reported in a similar energy range, although without any independent determination of the nanotube structure (as was provided by Rayleigh scattering in our studies). In contrast to these data,[8,10] we do not observe the strong phonon sideband peaks that have been reported to appear with nearly equal intensities to the main electronic transitions. We also fail to see evidence of features associated with free-carrier interband transitions.

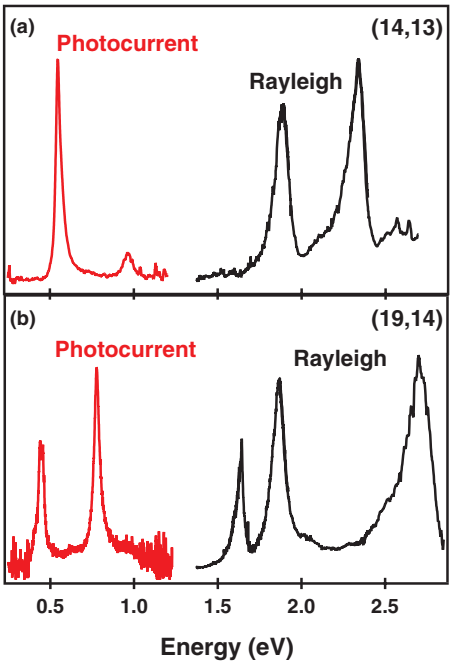

FIG. 2. (Color) Combined photoconductivity and Rayleigh scattering spectra for an individual single-walled nanotube. (a) For a (14,13) nanotube, showing the lowest four electronic transitions, E_{11}, E_{22}, E_{33}, and E_{44}. (b) For a (19,14) nanotube, showing the lowest five transitions, E_{11}, E_{22}, E_{33}, E_{44}, and E_{55}.

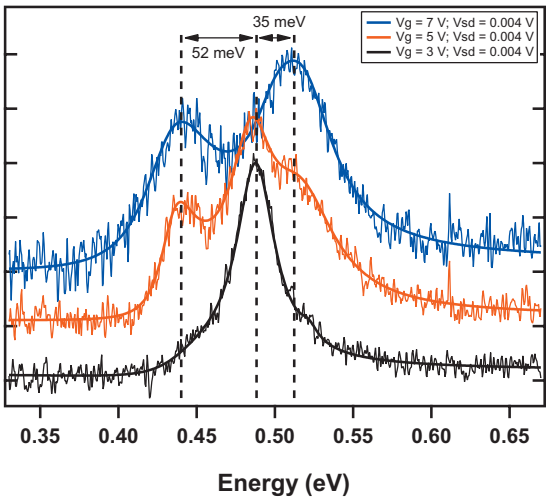

FIG. 3. (Color) Evolution of the photocurrent lineshape as a function of gate voltage. The spectra were sequentially collected from the lowest gate voltage (3 V) to the highest (7 V) and then again as the voltage is lowered to verify reproducibility.

Varying the applied gate voltage changes the lineshape of the low-energy feature while the average spectral position remains relatively constant, as shown in Fig. 3. As the gate voltage increases, we see new peaks on the wings of the low bias feature that eventually dominate the spectral response. The features were reproducible upon repeated gate sweeps. While the origin of these additional features is unknown, there are two physical effects that likely contribute. First, Freitag *et al.*[18] have shown that for similar three terminal SWNT devices, the Schottky barrier width and resulting electric field near the metal contact is modulated by the gate bias. Second, electrostatic doping will lead to additional free-charge carriers in the bulk of the SWNT. We note that a similar spectral lineshape variation was observed from the same SWNT at different contact positions, also likely reflecting changes in the spontaneous electric field distribution. Our interpretation of the energy scaling behavior is unaffected by this small lineshape variation.

TABLE I. Summary of SWNT transition energies measured by Fourier transform photoconductivity (E_{11},E_{22}) and Rayleigh scattering (E_{33},E_{44}).

(n,m)	d_t	E_{11}	E_{22}	E_{33}	E_{44}
(14,13)	1.86	0.55	0.96	1.89	2.34
(19,14)	2.28	0.45	0.78	1.64	1.87
(17,12)	2.00	0.53	0.92	1.89	2.18
(18,13)	2.14	0.48	0.84	1.76	2.03

Combining the FTPC spectra with the Rayleigh scattering spectra allows us to obtain, for the first time, broadband optical spectra of SWNTs of known chiral index over a broad spectral range, extending from 0.3–2.7 eV. For the (14,13) SWNT [Fig. 2(a)], this permits identification of the lowest four optical transitions (E_{11}=0.55, E_{22}=0.96, E_{33}=1.88, and E_{44}=2.33 eV). In the case of the (19,14) SWNT [Fig. 2(b)], a total of five optical transitions (up to E_{55}) are observed within our spectral window. The measured energies for the four lowest-lying electronic transitions for several individual SWNTs are presented in Table I.

Our data allow us to examine quantitatively the electronic structure of SWNTs in the large diameter limit. These results give us access to states corresponding to small values of the graphene wave vector, which is given by p/d_t, where p=1, 2, 4, and 5 for transitions E_{11}, E_{22}, E_{33}, and E_{44}, respectively. From our data, we find transition energy ratios for E_{22}/E_{11}, E_{33}/E_{11}, and E_{44}/E_{11} of 1.75, 3.5, and 4.25 (with a variation in $<\pm 3\%$ for the different nanotubes). Deviation from the values of 2, 4, and 5 predicted by single-particle theory (in the chiral-independent limit) provides further evidence for the importance of excitons and other many-body interactions.[27,28] Our experimentally determined energy ratios agree well with the values of 1.79, 3.44, and 4.23 for E_{ii}/E_{11} (i=2,3,4) calculated[12] for an artificial (15,15) semiconducting SWNT using an *ab initio* method with many-body effects.

In contrast, the transition energies that we have measured deviate significantly from trends observed for small diameter nanotubes. Figure 4 shows a plot of the widely used analytical 2D expression for the transition energy of near armchair nanotubes,[12] $a\frac{p}{d_t}[1+b\log\frac{c}{p/d_t}]$, with a, b, and c representing adjustable parameters and the log term representing the effects on the transition energies of electron-electron interactions. The curve in the figure has been reproduced directly from the work of Araujo *et al.*[29] in which the parameters are fit to measured optical transitions, corrected for chiral effects, in small diameter nanotubes; some of the original data are indicated as small squares (⊞). The figure also shows our results on large diameter nanotubes. The measured E_{22} transitions in Fig. 4 are seen to overlap in wave vector (p/d_t) with the E_{11} transitions for the smaller diameter nanotubes. However, the transition energies for the E_{11} transitions in the larger diameter nanotubes are ~15% lower. Likewise, the measured E_{11} values fall below the extrapolated 2D fit. As transition energies are weakly dependent on the nanotube chirality (even in the single-particle limit) a correction, proportional to $\cos 3\theta/d_t^2$, is typically applied to strictly examine the effects of diameter. While this correction can be significant for small radius tubes, we have found it to be negligible for the low-energy transitions of our large diameter SWNTs (<10 meV contribution for E_{11} and E_{22}). It is important to note that although differences exist in the dielectric environment under which these measurements were made, i.e., micellar solution versus an oxide surface, this effect alone cannot account for the discrepancy. Recent work has explicitly examined the effect of dielectric screening on the transition energies of excitons in SWNTs,[30] and has concluded that the shift in energy saturates rather quickly above ε_{env}=5. The maximum effect observed by the authors in this energy range is too small to account for our observed differences of ~120 meV.

A related breakdown of scaling was recently identified[16,29] for higher energy transitions (E_{33} and E_{44}). In these instances, the measured energies were also found to be incompatible with the scaling of the E_{11} and E_{22} transitions in smaller diameter SWNTs. This effect was ascribed to a diminished role of excitonic interactions for the higher-lying transitions. However, this explanation is not appropriate for the present breakdown in scaling, as it is observed within the system of E_{11} and E_{22} transitions for which the excitonic character has been well established.[20,21] Also, in contrast to the situation for higher energy transitions, where an overall blue-shift was observed for larger diameter nanotubes, the E_{11} and E_{22} transitions are found to lie lower in energy than the transitions associated with the same wave vector in the smaller diameter SWNTs. This effect can hardly be explained by the lack of excitonic interactions. We conclude

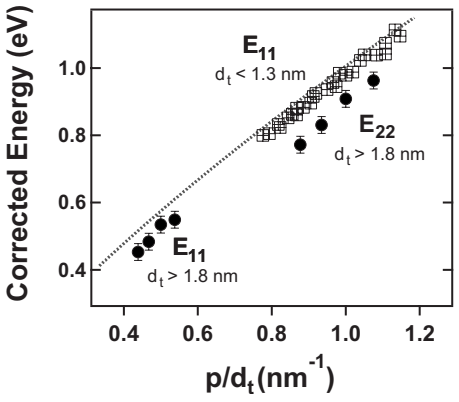

FIG. 4. Optical transition energies from large diameter SWNTs (filled dots) and from chiral corrected small diameter SWNTs (⊞) along with the extrapolated fit to a 2D many-body expression (dotted line) reproduced from Ref. 29. Low-energy transitions which originate from states with similar wave vectors show different energy dependence as a function of diameter.

that while the 2D model for nanotube optical transitions provides an elegant framework for a general understanding of nanotube transition energies and a surprisingly good quantitative description of transition energies for a limited range of structures and subbands, discrepancies in excess of 15% arise in applying the model to a broad range of nanotube diameters. In addition to the fundamental interest in this result, it is has important implications for the interpretation of spectroscopic data. Application of scaling theory calibrated for small diameter nanotubes to the analysis of optical spectra of low-lying transitions in large diameter nanotubes will lead to significant errors in the inferred nanotube diameter.

IV. CONCLUSIONS

We have demonstrated that the Fourier transform photoconductivity technique can be used to determine the band-gap energies of individual large diameter single-walled carbon nanotubes. Furthermore, all evidence points toward excitonic resonances including the lineshape, collection efficiency and scaling behavior between the E_{11} and E_{22} transitions. When combined with optical spectroscopy, an extremely broadband characterization of the electronic structure of a SWNT can be achieved.

ACKNOWLEDGMENTS

We thank Mark Hybertsen, Deborah Prezzi, and C. Kane for valuable discussion and R. Smith for technical assistance on the beamline. This manuscript has been authored by employees of Brookhaven Science Associates, LLC under Contract No. DE-AC02-98CH10886 with the U.S. Department of Energy (DOE). Research at Columbia University was supported by the DOE under Grant No. DE-FG02-03ER15463, the Nanoscale Science and Engineering Initiative of the NSF under Awards No. CHE-06-41523 and No. ECS-05-07111, by the Nanoelectronics Research Initiative (NRI) of the Semiconductor Research Corporation, and by the New York State Office of Science, Technology, and Academic Research (NYSTAR). The synchrotron studies were supported by the National Synchrotron Light Source and the Center for Synchrotron Biosciences, Case Western Reserve University, under Grant No. P41-EB-01979 with the National Institute for Biomedical Imaging and Bioengineering.

*Corresponding author; misewich@bnl.gov

†Present address: Laboratoire Pierre Aigrain, Ecole Normale Superieure, 24 rue Lhomond, Paris, France.

[1] A. Jorio, R. Saito, J. H. Hafner, C. M. Lieber, M. Hunter, T. McClure, G. Dresselhaus, and M. S. Dresselhaus, Phys. Rev. Lett. **86**, 1118 (2001).

[2] A. Hartschuh, H. N. Pedrosa, L. Novotny, and T. D. Krauss, Science **301**, 1354 (2003).

[3] J. Lefebvre, J. M. Fraser, P. Finnie, and Y. Homma, Phys. Rev. B **69**, 075403 (2004).

[4] M. Y. Sfeir, F. Wang, L. Huang, C.-C. Chuang, J. Hone, S. P. O'Brien, T. F. Heinz, and L. E. Brus, Science **306**, 1540 (2004).

[5] *Carbon Nanotubes: Advanced Topics in the Synthesis, Structure, Properties and Applications, Topics in Applied Physics*, edited by A. Jorio, G. Dresselhaus, and M. S. Dresselhaus (Springer, Berlin, Heidelberg, 2008), Vol. 111.

[6] G. D. Scholes and G. Rumbles, Nature Mater. **5**, 683 (2006).

[7] M. S. Dresselhaus, G. Dresselhaus, R. Saito, and A. Jorio, Annu. Rev. Phys. Chem. **58**, 719 (2007).

[8] A. D. Mohite, P. Gopinath, H. M. Shah, and B. W. Alphenaar, Nano Lett. **8**, 142 (2008).

[9] M. Freitag, Y. Martin, J. A. Misewich, R. Martel, and Ph. Avouris, Nano Lett. **3**, 1067 (2003).

[10] J. U. Lee, P. J. Codella, and M. Pietrzykowski, Appl. Phys. Lett. **90**, 053103 (2007).

[11] M. Y. Sfeir, T. Beetz, F. Wang, L. Huang, X. M. Henry Huang, M. Huang, J. Hone, S. O'Brien, J. A. Misewich, T. F. Heinz, L. Wu, Y. Zhu, and L. E. Brus, Science **312**, 554 (2006).

[12] C. L. Kane and E. J. Mele, Phys. Rev. Lett. **93**, 197402 (2004).

[13] E. H. Haroz, S. M. Bachilo, R. B. Weisman, and S. K. Doorn, Phys. Rev. B **77**, 125405 (2008).

[14] L. M. Huang, B. White, M. Y. Sfeir, M. Huang, H. X. Huang, S. Wind, J. Hone, and S. O'Brien, J. Phys. Chem. B **110**, 11103 (2006).

[15] S. M. Bachilo, M. S. Strano, C. Kittrell, R. H. Hauge, R. E. Smalley, and R. B. Weisman, Science **298**, 2361 (2002).

[16] T. Michel, M. Paillet, J. C. Meyer, V. N. Popov, L. Henrard, and J. L. Sauvajol, Phys. Rev. B **75**, 155432 (2007).

[17] X. M. H. Huang, R. Caldwell, L. Huang, S. C. Jun, M. Huang, M. Y. Sfeir, S. P. O'Brien, and J. Hone, Nano Lett. **5**, 1515 (2005).

[18] M. Freitag, J. C. Tsang, A. Bol, D. Yuan, J. Liu, and P. Avouris, Nano Lett. **7**, 2037 (2007).

[19] P. R. Griffiths and J. A. de Haseth, *Fourier Transform Infrared Spectrometry, Chemical Analysis* (Wiley, New York, 1986), Vol. 83.

[20] F. Wang, G. Dukovic, L. E. Brus, and T. F. Heinz, Science **308**, 838 (2005).

[21] J. Maultzsch, R. Pomraenke, S. Reich, E. Chang, D. Prezzi, A. Ruini, E. Molinari, M. S. Strano, C. Thomsen, and C. Lienau, Phys. Rev. B **72**, 241402 (2005).

[22] S. Kazaoui (private communication).

[23] N. Kirova and S. Brazovskii, Synth. Met. **119**, 651 (2001).

[24] S. Berciaud, L. Cognet, and B. Lounis, Phys. Rev. Lett. **101**, 077402 (2008).

[25] F. Wang, G. Dukovic, L. E. Brus, and T. F. Heinz, Phys. Rev. Lett. **92**, 177401 (2004).

[26] A. Hagen, M. Steiner, M. B. Raschke, C. Lienau, T. Hertel, H. Qian, A. J. Meixner, and A. Hartschuh, Phys. Rev. Lett. **95**, 197401 (2005).

[27] C. L. Kane and E. J. Mele, Phys. Rev. Lett. **90**, 207401 (2003).

[28] H. Zhao and S. Mazumdar, Phys. Rev. Lett. **93**, 157402 (2004).

[29] P. T. Araujo, S. K. Doorn, S. Kilina, S. Tretiak, E. Einarsson, S. Maruyama, H. Chacham, M. A. Pimenta, and A. Jorio, Phys. Rev. Lett. **98**, 067401 (2007).

[30] Y. Miyauchi, R. Saito, K. Sato, Y. Ohno, S. Iwasaki, T. Mizutani, J. Jiang, and S. Maruyama, Chem. Phys. Lett. **442**, 394 (2007).